

Characterization and Performance of the Suomi-NPP VIIRS Solar Diffuser Stability Monitor

Fulbright, Jon P.*^a, Lei, Ning^a, Chiang, Kwofu^a, and Xiong, Xiaoxiong^b

^aSigma Space Corporation, 4600 Forbes Blvd., Lanham, MD, USA 20706

^bSciences and Exploration Directorate, NASA Goddard Space Flight Center, Greenbelt, MD, USA 20771

ABSTRACT

We describe the on-orbit characterization and performance of the Solar Diffuser Stability Monitor (SDSM) on-board Suomi-NPP/VIIRS. This description includes the observing procedure of each SDSM event, the algorithms used to generate the Solar Diffuser degradation corrective factors, and the results for the mission to date. We will also compare the performance of the VIIRS SDSM and SD to the similar components operating on the MODIS instrument on the EOS Terra and Aqua satellites.

Keywords: NPP, VIIRS, on-orbit, calibration

1. INTRODUCTION

The primary calibration coefficient of the Reflected Solar Bands (RSB; 0.4-2.3 μm) in VIIRS is the so-called F-factor. The F-factor is computed using observations of the Solar Diffuser (SD) while it is fully illuminated by the Sun. Alternative calibration methods exist, but observations of the SD are the principal method of determining F-factors.¹

The Solar Diffuser view of VIIRS is made up of a pinhole light-attenuating screen and a diffusing panel of Spectralon[®] (produced by Labsphere, Inc.). The surface of Spectralon has high reflectivity with near-Lambertian light diffusion properties². The reflectivity of Spectralon, however, degrades with exposure to UV light. The degradation for a given exposure of UV light is greatest at shorter wavelengths (“yellowing”) and is minimal at wavelengths longer than about 900 nm³. The degradation of reflectivity of the SD panel is a vital parameter of the SD calibration.

The amount of degradation is quantified as the H-factor. The H-factor is a multiplicative constant onto the initial Bi-directional Reflectance Distribution Function (BRDF) of the SD panel ($\text{BRDF}(t) = H(t) \cdot \text{BRDF}_0$). An H value of 1 means no degradation since the prelaunch measurement, while an H value of 0 means no light is being reflected in that band. The H-factor is calculated for RSB bands M1 through M7, as well as for the bands I1 and I2. The reflective SD panel is not expected to degrade significantly in the near-IR (beyond ~900 nm).

The design of VIIRS includes an instrument that measures the BRDF as the mission progresses. The Solar Diffuser Stability Monitor (SDSM) is a ratioing radiometer that operates while the Sun illuminates the SD panel. This design is very similar to the system used in the MODIS instruments⁴. The main part of the SDSM is an integrating sphere that contains eight detectors. These eight detectors are filtered to measure 8 wavelength bands, seven of which have the same wavelength centers as the RSB bands M1-M7, and the eighth has a band pass centered at 935 nm⁵. Table 1 lists the band centers for these eight detectors. An internal mirror alternates the input for the integrating sphere between views of the SD, of a direct view of the Sun (through a ~0.1% attenuation screen) and of a dark cavity inside the SDSM. The analysis of the data collected by the SDSM during its operation can be used to determine the change in the BRDF of the SD as a function of time. A schematic of the SDSM and its functional relationship to the VIIRS optical light path is given in Figure 1.

As can be seen in Figure 1, the SDSM samples light coming from the SD at only one view angle. One of the assumptions in the definition of the H-factor is that the shape of the BRDF as a function of angle does not change with time. More specifically, the assumption is that the BRDF as seen from the rotating telescope assembly, and therefore the main VIIRS detectors, degrades at the same rate as the BRDF as seen from the SDSM.

*jon.fulbright@sigmaspace.com; phone 1 301 552-5288; fax 1 301 552-5222; sigmaspace.com

In Section 2 of this paper, we describe the methodology we use to determine the H-factors. We also discuss the degradation of the SDSM detectors and explore a rough estimate of the uncertainty in the H-factors. In Section 3, we explain our method for finding the long-term trending of the H-factors via exponential fitting as well as improving the uncertainty estimates of the H-factors.

Table 1. SDSM detector band centers and related VIIRS bands.

Detector	Band Center	VIIRS Bands
1	412 nm	M1
2	445 nm	M2
3	488 nm	M3
4	555 nm	M4, I1
5	672 nm	M5, I1
6	746 nm	M6
7	865 nm	M7, I2
8	935 nm	None

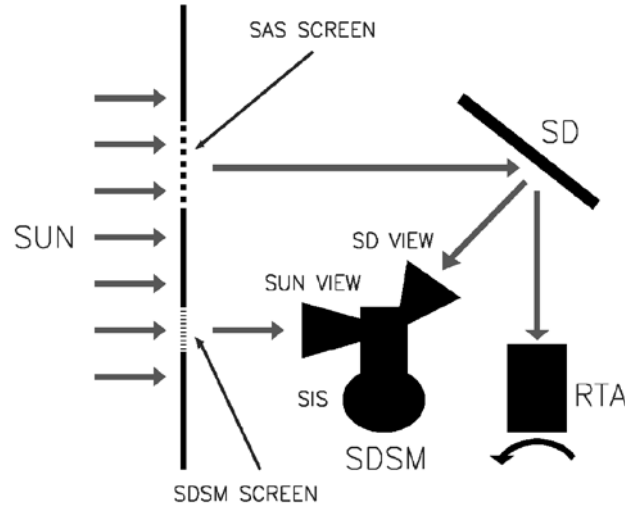


Figure 1. Schematic of the SDSM system within VIIRS (not to scale). An internal mirror within the SDSM (not shown) selects whether the internal integrating sphere (SIS) receives light from the Sun view direction, the Solar Diffuser (SD) view direction, or from a sealed dark cavity within the SDSM. Unlike the SDSM system on MODIS, the SAS screen is fixed.

3.

2. METHODOLOGY OF CALCULATING H-FACTORS

2.1 Background

As mentioned above, the SDSM is a ratioing radiometer. The degradation of the SD will result in a similar degradation of the response seen by the SDSM detectors while the internal mirror is pointing at the Sun-illuminated SD screen (the “SD view”) over time. This detector response can also be affected by other factors, such as spacecraft-Sun distance, temperature effects on the detector gain, and solar variations. Therefore, the SDSM detector response from the SD screen is normalized by the SDSM detector response while the internal mirror is pointed towards the direct Sun port (“Sun view”). The ratio of the response should be constant if there is no degradation, assuming the response is corrected

for the other measurable instrumental effects, namely the geometry-based corrections of the transmission screens and the cosine of the angle of incidence on the SD.

In order to eliminate dark current, the SDSM also records the response while the internal mirror points towards a dark cavity sealed from the rest of VIIRS. The response from this “dark view” is subtracted from the response obtained from the SD and Sun views. It should be noted that the SDSM is operated while Suomi/NPP is on the night-side of the Earth, which helps minimize the amount of stray light entering the SDSM at the other mirror positions.

The SDSM switches between the three different views sequentially between scans. That is, one scan the internal mirror is pointing at the SD view, then for the next scan the mirror points toward the Sun view, then toward the dark view on the third scan, and finally back to the SD view as the three-scan cycle begins again. During each scan the SDSM records 5 samples from each of its detectors. Each set of three scans is called a “scan triple” and is the basic unit of the data reduction.

An example of the data recorded by the SDSM during a normal event is show in Figure 2. These data were recorded on November 8, 2011 on Orbit 154 during the Intensive Cal/Val period. The SDSM was operated for 8 minutes (rather than the nominal 2 minute activation) to ensure the SDSM was operating during the period when both the SD and the Sun views were fully illuminated by the Sun. This period of full illumination is called the “sweet spot” of the observation and is marked on the figure. In this example, there are only four scan triples that fulfill the solar angle requirements. There can be up to approximately 10 good scan triples for each SDSM event, depending on the time of year. The variation is due to a small misalignment of the orientation of the SDSM Sun view that for some solar azimuth angles effectively shortens the time when both views are fully illuminated. The example given in the figure was taken from such a time to illustrate the effect of the misalignment.

Due to a design error, the Sun view response data from the MODIS SDSM contains “ripples” as a function of solar angle.⁶ This is not seen in the VIIRS data. The nearly flat SDSM response during the sweet spot period means that we will not have to rely on the data analysis method developed for MODIS data where the response is normalized by the red-most detector response.

2.2. H-factor calculation algorithm

The H-factors are determined by comparing the irradiance measurements from the Sun view and the SD view and tracking how they change over time.⁷ The irradiance of the SD view can be quantified as:

$$E_{SD} = G \cdot dc_{SD} = \cos \theta_{inc} \cdot \frac{\Phi_{sun}}{4\pi d_{sun}^2} \cdot \tau_{SD} \cdot \Omega_{SDSM} \cdot BRDF(t) \quad (1)$$

where G = SDSM detector gain, dc_{SD} is the dark-corrected detector response, θ_{inc} is the angle of incidence onto the SD screen, Φ_{sun} is the spectral output power of the Sun ($W/\mu m$), d_{sun} is the NPP-Sun distance, τ_{SD} is the transmittance of the screen in front of the SD, Ω_{SDSM} is the solid angle defined by the SD viewing cone, and $BRDF(t)$ is the time-dependent BRDF function—the quantity we wish to determine. Note all of the quantities on the right side of the equation except for Φ_{sun} , d_{sun} , and Ω_{SDSM} are dependent on the geometry of the solar light incident on the spacecraft. Also, Φ_{sun} and $BRDF(t)$ are band-dependent.

The irradiance of the Sun view can be quantified as:

$$E_{Sun} = G \cdot dc_{Sun} = \frac{\Phi_{Sun}}{4\pi d_{Sun}^2} \cdot \tau_{Sun} \quad (2)$$

As before, gain and τ_{Sun} are wavelength-dependent, and τ_{Sun} is dependent on the angle incident on the Sun view screen.

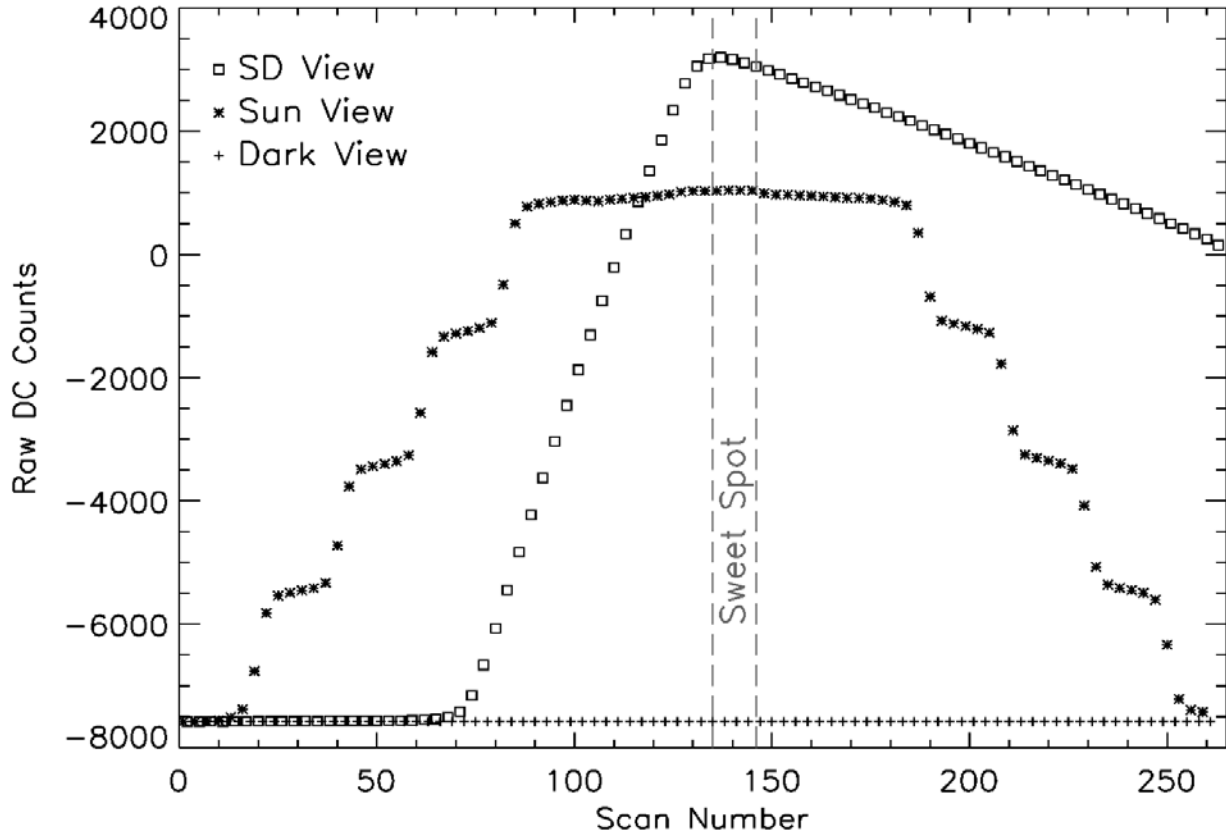


Figure 2. Raw DC counts from the SDSM event from Orbit 154 on November 8, 2011. Only the data from SDSM Detector 5 is presented here, but the other seven detectors show the same pattern. The SDSM was operated for 8 minutes to ensure there was data recorded during the period where both the Solar Diffuser and the Sun View ports were fully illuminated (marked on this plot as the “sweet spot”). For this event, there were 4 “scan triples” recorded during this full-illumination period. A scan triple consists of three consecutive scans where the SDSM mirror spends one scan each observing the dark view, SD view and Sun view. The bright spots seen in the MODIS SDSM Sun view data are not present in the VIIRS data.

If we take the two equations and divide E_{SD} by E_{Sun} , then solve for $BRDF(t)$, we then obtain:

$$BRDF(t) = \frac{\tau_{Sun} \cdot dc_{SD}}{\tau_{SD} \cdot \Omega_{SDSM} \cdot \cos \theta_{inc} \cdot dc_{Sun}} \quad (3)$$

The detector gain, G , and the solar flux factor cancel out. Remember that $BRDF(t) = H(t) \cdot BRDF_0$, so we can then solve for $H(t)$:

$$H(t) = \frac{\tau_{Sun} \cdot dc_{SD}}{\tau_{SD} \cdot \Omega_{SDSM} \cdot \cos \theta_{inc} \cdot dc_{Sun} \cdot BRDF_0} \quad (4)$$

In practice, the value of $H(t)$ is computed using h-factors:

$$\frac{H(t_i)}{H(t_j)} = \frac{h_j}{h_i} \quad (5)$$

Where the subscripts i and j refer to two different SDSM events. This ratio method reduces the functional dependencies on (near) static instrumental parameters. The value h is what is calculated by the practical code. Its value is defined by:

$$h(t_i) = \frac{1}{N_i} \sum_{n=1}^{n=N_i} BRDF_0 \cdot \cos \theta_{inc} \cdot \frac{dc_{Sun} \cdot \tau_{SD}}{dc_{SD} \cdot \tau_{Sun}} \quad (6)$$

where N_i is the number of samples within the scan triples used in the analysis. All of the factors within the summation are recalculated for each term in the sum. While not explicitly stated in the above equation, the values for the $BRDF_0$, τ_{SD} and $\cos \theta_{inc}$ are calculated for the view angles at the exact time the samples of the SD view are taken. Similarly, τ_{Sun} is calculated for when the samples of the Sun view are taken.

For a given SDSM “event” (the entirety of the SDSM operations for a given orbit), the analysis code finds all the scan triples, calculates the solar angles in the various coordinate systems, and determines if the scan triple will be used in the h-factor calculation. If so, the necessary values are derived from the LUTs and the h-factor for that event is calculated using Equation 6. The h-factor for each band and the data (both measured and derived) are saved into an IDL save file referencing this SDSM event for future calculations.

2.3. Timing considerations

The look-up tables (LUTs) that give the $BRDF_0$, τ_{SD} , and τ_{Sun} are angle-dependent. The dc values for a given sample correspond to a specific time, and the angles used for the LUT inputs for that sample should be interpolated to that specific time. Therefore, some consideration must be made in understanding the specific timing of events with regard to what is recorded in the OBC-IP (On-Board Calibrator-Intermediate Product) files.

The time given in the OBC-IP file for each scan is the “EV_START_TIME”, which is the IET time at the start of the Earth View sampling. The solar position vector given in the OBC-IP files is recorded at the time the SD observations are made by the main VIIRS detectors, which is 1.057 s after the EV_START_TIME. The five SDSM samples occur at roughly 0.1 s intervals slightly after the VIIRS detectors view the SD. The exact relative times of the SDSM samples are given in the “Solar Diffuser SDSM Time” LUT. The first SDSM sample takes place 1.108 s after EV_START_TIME. The solar elevation (vertical) angle changes by about 0.018 deg in 0.1 s (or about 0.3 deg over a course of a scan), while the azimuth (horizontal) angle changes by only about a tenth as much in the same time period. The largest effect is on the results from the vignetting functions and the initial value of the BRDF: the values can change by up to 0.03 percent each in 0.1 s, which is non-negligible given the quality of the data taken by the SDSM and the uncertainty requirements of the determination of H-factors.

2.4. Detector response trending

The corrected, normalized SDSM response from the Sun view and SD view are shown in Figure 3. The plotted values are the result of solving Equations 1 and 2 for $1/G$, or the inverse gain. Normalizing to the first SDSM event eliminates the constants (such as Ω_{SDSM}) from the calculation.

The response from the Sun view, which theoretically should be nearly constant, shows a marked decrease in several of the passbands. This behavior is also seen in the MODIS SDSM detectors. While the nature of the degradation of the detector response is not fully understood, the form of the degradation is similar to what would be expected if some kind of particle radiation, most likely protons from the Sun, was affecting the detectors.⁸ For example, the degradation continues even over periods where the SDSM was not operating (such as around Orbits 800-1000). If the degradation was related to exposure to solar UV light, for example, as are the VIIRS mirrors, the degradation would stop when the SDSM is not operated. The SDSM mirror points to the dark cavity when the SDSM is not operating, sealing off the detectors from outside light.

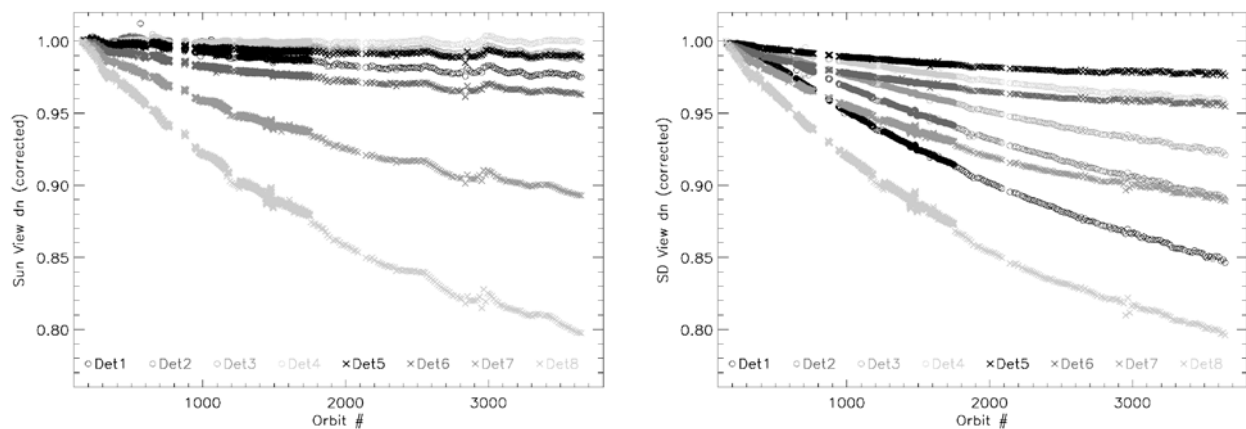


Figure 3. Normalized and corrected detector responses from the Sun view (left) and SD view (right). The nature of the corrections is given in the text. The Sun view data show the effects of the SDSM detector degradation over the course of the mission as well as the effects of unresolved structures in the Sun view vignetting function (for example, the feature around Orbit 3000). The SD view response data shows both the effects of the SDSM detector degradation and the degradation of the SD. Compare, for example, the degradation of the Detector 1 response between the two panels. Detector 1, with a passband centered at 412 nm, should show the largest effects from the degradation of the Solar Diffuser of any of the SDSM detectors. Also note the feature around Orbit 1500. This feature occurs at the time of a VIIRS Warm-up/Cool-down cycle and is the result of the temperature sensitivity.

3. RESULTS

3.1 H-factors

The H-factors for approximately the first 10 months of the mission are shown in Figure 4. Several features are apparent in the data. First, there are several gaps in the data, especially around orbits 500-1000. These include some periods when the VIIRS operations were shut down in order to study the response anomaly of the VIIRS mirrors. The degradation of the SD continued over this period because, unlike MODIS, there is no movable door protecting the SD when it is not in use.

Second, the degradation trend appears different during approximately the first 150 orbits of operation (before Orbit 289). The star tracking data for this early mission time was inaccurate, which leads to errors in the solar angles used in the H-factor calculations. These early-mission data are not used in the trending analysis.

Finally, there are some “bumps” in the data that appear in all eight bands. These same deviations are seen in the Sun view response data and are caused by our imperfect knowledge of the vignetting function of the Sun view screen. We are using a vignetting function created from on-orbit data⁹ that is best-defined through Orbit 1750. A future update that contains an improved vignetting function through the solar angles covered by the more recent orbits should remove most of the features since Orbit 1750.

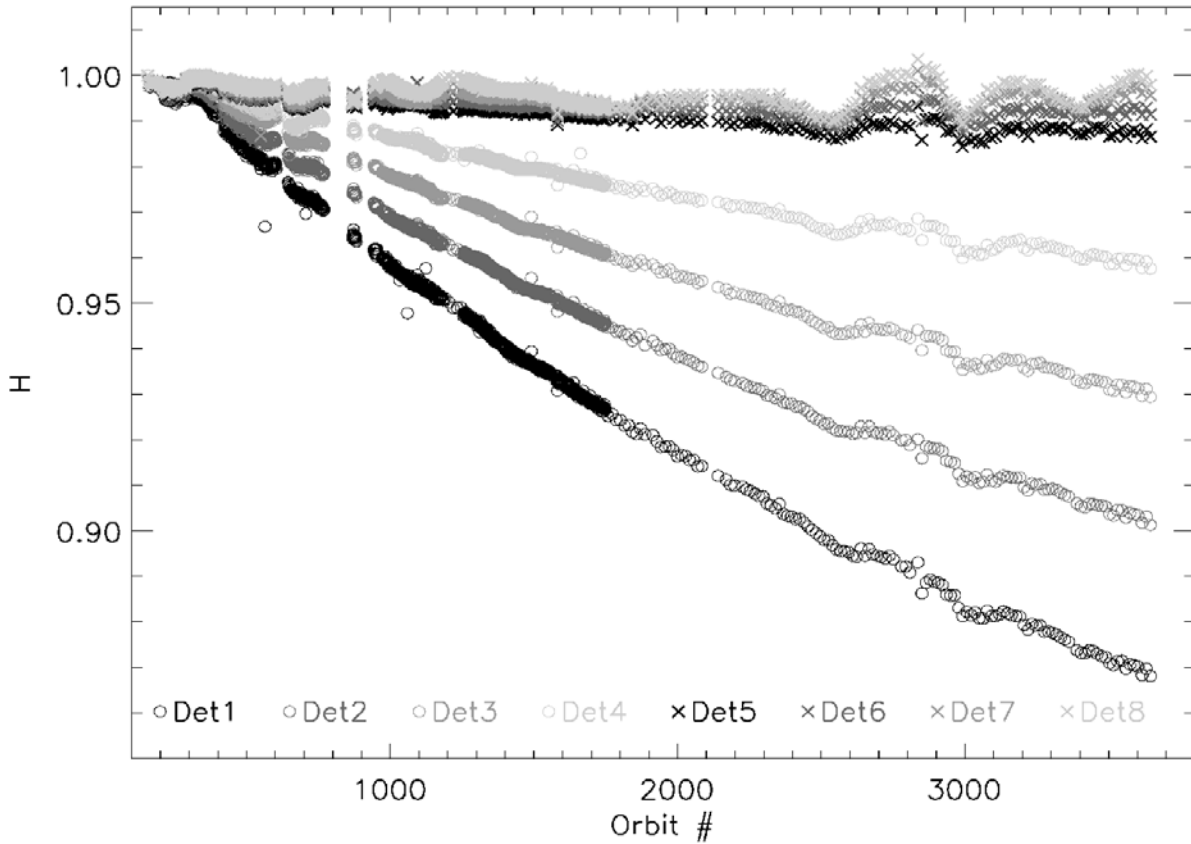


Figure 4. H-factors for approximately the first 10 months of the Suomi/NPP mission for all eight SDSM bands. Many of the features in the H-factor trends seen in the data are described in the text. These features include gaps in the data due to intentional or accidental instrument/spacecraft shutdowns. Also before Orbit 345 the H-factor calculations were adversely affected by lower-quality spacecraft pointing data. Finally, the undulations in the data after Orbit 1750 are due to unresolved variations in the Sun view attenuation screen.

3.2. Uncertainty in the SDSM observations

The uncertainty in the H-factor is based on our imperfect knowledge of the inputs in Equation 6: the response from all three views, the solar angle, the initial BRDF value at the solar angle, and the transmission of the two screens at the solar angle. By far, the greatest uncertainty in our calculation of the H-factors is our lack of knowledge of the transmission through the two screens, especially through the Sun View screen. The pre-launch LUT for τ_{Sun} is given in 2 degree increments in azimuth and 0.15 degree increments in elevation. The on-orbit determination of τ_{Sun} shows features in the transmission function that are unresolved by the pre-launch table. Continued improvement of τ_{Sun} (as well as τ_{SD}) determined by on-orbit observations should greatly reduce the observational uncertainties.

The Signal-to-Noise Ratio (SNR) of the SDSM response is sufficiently high that uncertainty from the response does not contribute significantly to the overall uncertainty of the H-factors. In Figure 5, exponential fits to SNR ratio for both the Sun view and SD view response for each SDSM event are plotted as a function of orbit. The fit values are shown than the raw SNR data because of the large (40%) orbit-to-orbit variations in the SNR value. This large variability is not a sign of poor quality data, rather it is indicative of the problem of quantifying the SNR value when it is so high and the number of data samples is small (5-20 samples). Indeed, there are a few cases where all 5 samples for a given orbit are identical, which means the noise for that observation is at the quantization error limit.

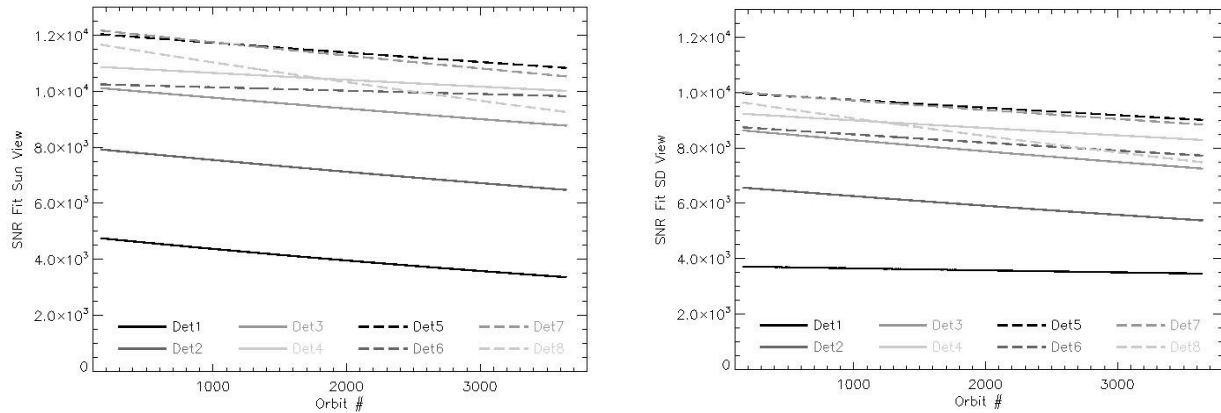


Figure 5. Best-fit SNR values for the Sun view (left) and SD view (right) detector response for all eight SDSM bands. As explained in the text, the SNR values vary greatly orbit-to-orbit, so only the exponential fit to the data for a given band is plotted here. The SNR values are extremely high, even given the degradation of the SDSM detectors. If the effect of the detector degradation continues to produce the same exponential drop off, the end-of-mission SNR values will still be adequate to determine the H-factors.

The SNR is dropping due to the degradation of the SDSM detectors, but at this time the SNR ratios are extremely high. The expected contribution of the uncertainty in the response is far below the observed event-to-event scatter seen in the H-factors. The SNR levels should stay at this high level throughout the Suomi/NPP mission lifetime if the present trends of detector degradation continue.

An estimate of the uncertainty in the H-factor can be made by noting that the h-factor for a given orbit is just the average of the individual scan triple results (Equation 6). In that case, the standard deviation of the mean describes the uncertainty in the h-factor, assuming that the uncertainties in each observation used in the mean are normally distributed. The uncertainty in the H-factor can then be determined using normal propagation of uncertainty rules, assuming each observation is independent. The resulting values of σ_H are plotted in Figure 6.

Neither of the assumptions used in the calculation of these uncertainty values may be valid, as the inputs for some of the major possible sources of error (such as the vignetting functions) are highly correlated scan-to-scan and orbit-to-orbit and are not random. There are often only 3 to 5 scan triples per SDSM event, so the results can also be affected by the small sample sizes. The orbit-to-orbit variation in the H-factors, as treated in the next section, is most likely a more reliable estimate of the uncertainty of our H-factor determinations. This method, however, does have use in diagnosing whether the H-factor determined by an individual orbit is reliable.

2.4. H-factor trending

The H-factors are defined with respect to each other by Equation 5. The SDSM was first operated at orbit 154, eleven days after NPP was launched. The SD screen was exposed to the Sun and had degraded since the time of launch, but we cannot directly determine the amount of degradation from the on-orbit data unless we assume the degradation follows a functional pattern.

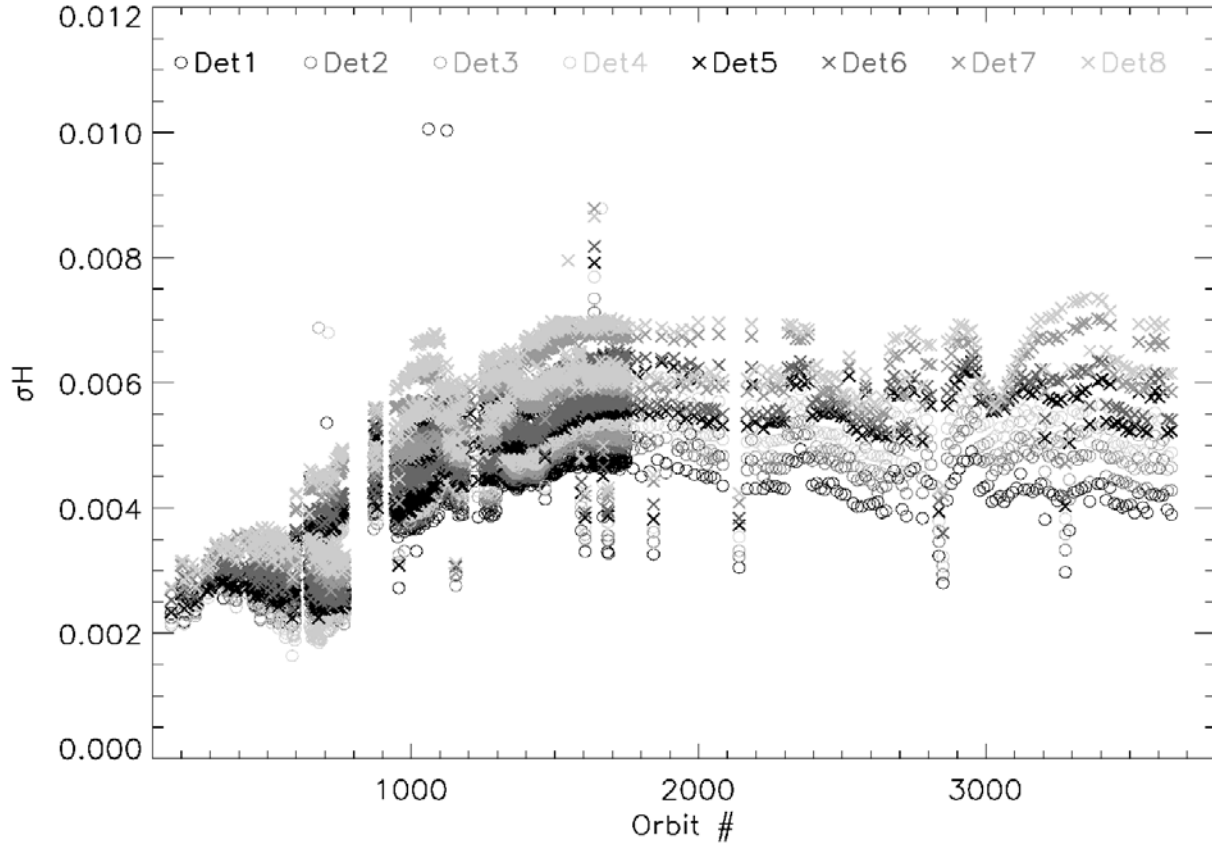


Figure 6. Estimate of the uncertainty of the H-factors shown in Figure 5 using the method described in Section 2.3. This method utilizes the standard deviation of the mean for the h-factor calculation in Equation 6.

$$H(t) = e^{(a_0 + a_1 \cdot t + a_2 \cdot t^2)} \quad (7)$$

The MODIS instruments on Aqua and Terra have a SD and SDSM calibration system very much like the system on VIIRS. It has been found that the H-factor trending for MODIS is well-fit by a quadratic exponential of the form¹⁰:

$$H(t) = e^{(a_0 + a_1 \cdot t + a_2 \cdot t^2)} \quad (8)$$

We adopt this form for use with VIIRS. In the equation above, t is counted in days and $t = 0$ is set for the time of the launch (2455862.908333 JD). If we force $a_0 = 0$ and fit to the available H-factor data, we can derive the absolute H-factors relative to $H(0) = 1$.

To create the fit, we use Equations 5 and 6 to derive H-factors for each SDSM event. For the early part of the mission (most orbits before Orbit 1750), the SDSM was operated every orbit VIIRS was functioning (approximately 14.7 SDSM events per day). After that time, the SDSM has been operated once per day. To achieve statistical balance between these two modes of operation, we weight the once-per-day SDSM data points by a factor of 14.7 more than the once-per-orbit SDSM data.

The rescaled (e.g., H is 1 at the time of launch rather than at the first SDSM event on Orbit 156) H-factors and the fits are shown in Figure 7. The residuals of the fits are given in Figure 8, and the coefficients and fitting uncertainties are listed in Table 2.

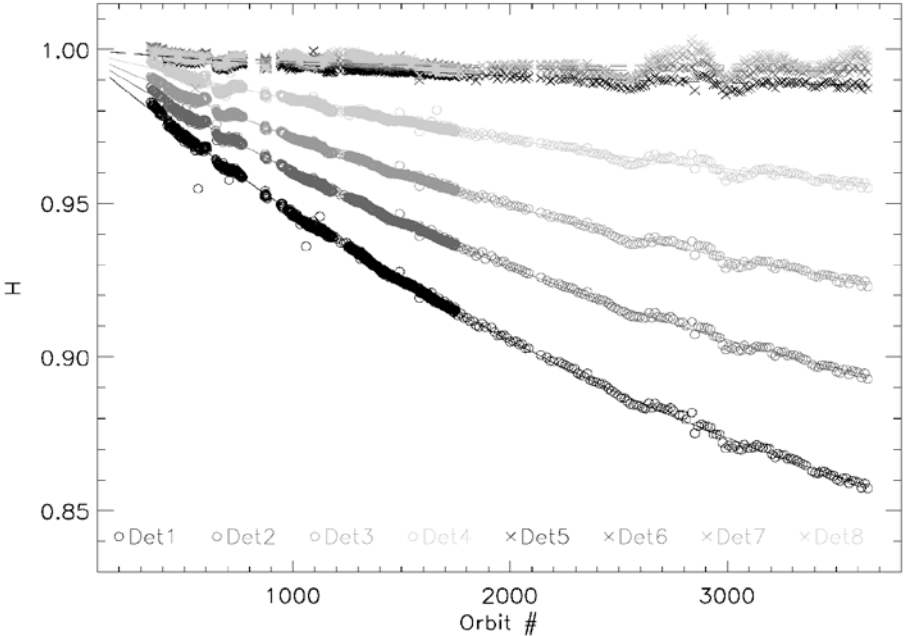


Figure 7. H-factors rescaled to H = 1 at launch and the fits to the H-factors.

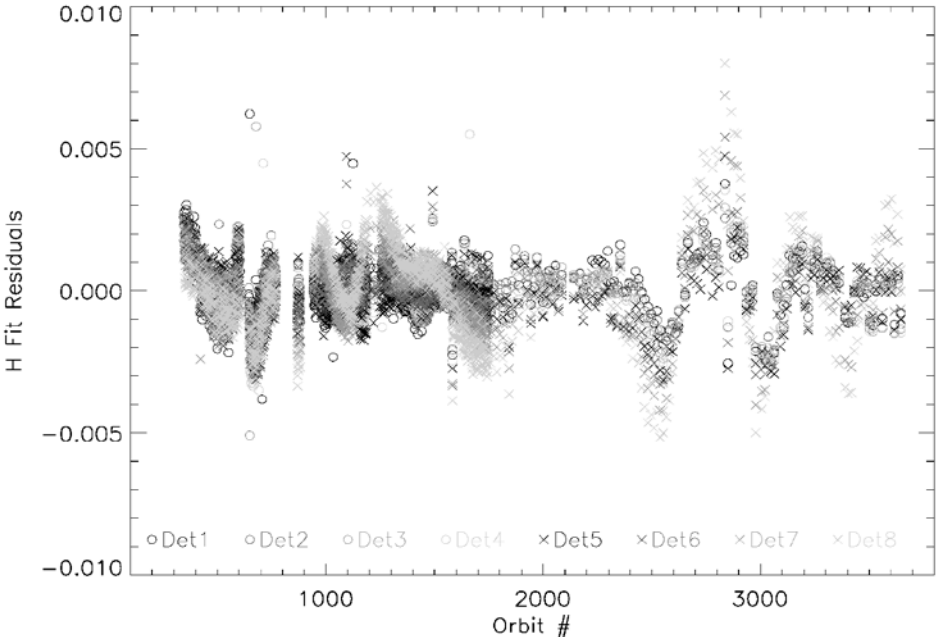


Figure 8. Residuals to the fits given in Figure 7. The largest residuals correspond to the features corresponding to uncertainties in the Sun view vignetting function. As can be ascertained from the data in Table 2, the variances in the residuals are much smaller than the estimates for the uncertainty in H shown in Figure 4.

Table 2. Coefficients of the fits to the H-factor data (see Equation 7). The coefficient a_0 is defined as equal to zero in all cases. The value of σ_{fit} is the standard deviation of the residuals of the fit for that detector. The σ_{fit} values are significantly lower than the σ_H values determined in Section 3.2, and are a more realistic estimate of our uncertainty in determining the H-factor trends.

Detector	a_1	a_2	σ_{fit}
1	-8.399×10^{-4}	9.493×10^{-7}	1.01×10^{-3}
2	-6.243×10^{-4}	7.320×10^{-7}	7.80×10^{-4}
3	-4.496×10^{-4}	5.573×10^{-7}	7.86×10^{-4}
4	-2.566×10^{-4}	3.245×10^{-7}	9.29×10^{-4}
5	-8.057×10^{-5}	1.377×10^{-7}	9.36×10^{-4}
6	-6.572×10^{-5}	1.586×10^{-7}	9.68×10^{-4}
7	-6.696×10^{-5}	2.034×10^{-7}	1.25×10^{-3}
8	-6.335×10^{-5}	2.005×10^{-7}	1.58×10^{-3}

4. SUMMARY

We have presented our methodology for determining the degradation of the Suomi/NPP VIIRS Solar Diffuser using the SDSM instrument. We have produced H-factors describing this degradation and estimates for these H-factors. The H-factor trends over the course of the mission are stable and well-fit by a quadratic exponential.

In comparison to the similar SDSM systems operating on the MODIS instrument on the EOS satellites Terra and Aqua, the SDSM system on VIIRS does not have the “ripples” in the Sun view response that severely affect the MODIS SDSM systems. All three SDSM systems show the same type of detector degradation at comparable rates. This bodes well for the long-term reliability of the NPP VIIRS SDSM system, and this conclusion is supported by our own trending of the response SNR and uncertainty measurements of the H-factors.

The most improvement in the H-factor results will come from the further development of the on-orbit vignetting function for the Sun view screen. At this point, a single quadratic exponential fit for each band describes the H-factor trends very well, but if the quality of the fit decreases, it may become necessary to fit the H-factors over separate time segments, as is done for the MODIS data.

REFERENCES

- [1] Mills, S., “VIIRS radiometric calibration algorithm theoretical basis document (section 3.3.3)”, tech report, Northrop Grumman (2010)
- [2] Robinson, B., Bliton, M., Menzel, R., Tyler, D., “Performance verification report – VIIRS FU1 reflective band calibration (PVP section 5.1)”, tech. rep., Raytheon (2009)
- [3] Bruegge, C. J., Stiegman, A. E., Rainem, R. A., and Springsteen, A. W., “Use of Spectralon as a diffuse reflectance standard for in-flight calibration of earth-orbiting sensors, *Optical Engineering*, **32**(04), 805-814 (1993)
- [4] Xiong, X., Sun, J., Barnes, W., Salomonson, V., Esposito, J., Erives, H., and Guenther, B., “Multiyear on-orbit calibration and performance of Terra MODIS reflective solar bands”, *IEEE Trans. Geosci. Remote Sen.* **45**(4), 879-889 (2007).
- [5] Robinson, B., Bliton, M., Menzel, R., Tyler, D., “Performance verification report – VIIRS FU1 reflective band calibration (PVP section 5.3)”, tech. rep., Raytheon (2009)
- [6] Xiong, X., Erives, H., Xiong, S., Xie, X., Esposito, J., Sun, J., and Barnes, W., “Performance of Terra MODIS solar diffuser stability monitor”, *Proc. of SPIE* **5882** (2005)
- [7] Mills, S., “VIIRS radiometric calibration algorithm theoretical basis document (section 3.3.3.1)”, tech report, Northrop Grumman (2010)
- [8] Eplee, G. private communication (?)
- [9] McIntire, J., Efremova, B., Moyer, D., Lee, S., and Xiong, X., “Analysis of Suomi-NPP VIIRS vignetting functions based on yaw maneuver data”, *Proc. of SPIE* this vol. (2012)
- [10] Choi, J., Angal, A., and Sun, J., “Terra MODIS SD degradation algorithm update”, tech report, MCST, (2007)